Design of high-power Nd:YAG solar laser pumped with off-axis parabolic concentrators

RABEH BOUTAKA[1,*], DAWEI LIANG[2], ROCHDI BOUADJEMINE[1], NORDINE HENDAOUI[1]
[1]*Centre de Développement des Technologies Avancées, Cité 20 Aout 1956, Baba Hassen, Alger, BP 17, Algérie*
[2]*CEFITEC, Departamento de Física, FCT, Universidade Nova de Lisboa, 2829-516, Portugal*

In this paper, we report a numerical study of high power Nd:YAG solar laser approach pumped through off-axis parabolic concentrators. Six off-axis parabolic mirrors with 15 m² total collection area were used to collect and focus the solar energy towards six 2V-shaped pump cavities, within which a 120 mm length, 7.5 mm diameter Nd:YAG laser crystal was transversally pumped. Six fused-silica lenses were also employed to efficiently couple the concentrated solar power with a laser rod. All pumping parameters of the laser design were optimized using the ZEMAX© non sequential ray-tracing method. The laser resonant cavity and its performance were analyzed by LASCAD© software. A maximum continuous-wave 1064 nm laser power of 646 W was numerically achieved in the multimode operation with high collection efficiency of 43.06 W/mm² and very small beam spot size. To the best of our knowledge, this is the highest laser output power from a single beam/single rod Nd:YAG solar laser scheme, which is more than 5 times that of the previous most powerful Nd:YAG solar laser. Moreover, the laser intensity at the focal plane was 2.85×10^6 W/cm², which can produce magnesium energy more than 14 times over the existing experimental works for laser-induced magnesium production.

(Received July 1, 2024; accepted December 2, 2024)

Keywords: Solid-state laser, Solar energy pumping, Nd:YAG, Off-axis concentrators, ZEMAX optimization, LASCAD analysis

1. Introduction

Given that solar energy is abundant and free in many countries worldwide like in Algeria [1-4], utilizing it as a pumping source to produce cost-effective laser systems is highly desirable, especially considering that conventional pumping sources such as flash lamps and laser diodes could result in higher costs. Furthermore, solar lasers can be employed to produce renewable energy by exploiting the chemical potential of magnesium through magnesium-oxide reduction [5-9]. In this way, a high-output power solar laser with high intensity at the focal region is required to enhance magnesium production, thereby improving the efficiency and economy of this renewable technology [6].

Since C. G. Young first achieved a 1 W continuous-wave (CW) output power solid-state solar-pumped laser in 1966 [10], numerous experimental and numerical studies have been conducted to enhance laser performance, particularly focusing on output power, efficiency, and beam quality [11-32]. In these works, significant progress was achieved in improving the performance of solar-pumped lasers by using different pumping schemes and different optical concentrators. For the single beam/single rod solar laser scheme, the most powerful solar laser was experimentally realized in 2012 [12], in this work 120 W CW multimode laser power was reached by pumping a 6 mm diameter, 100 mm length Nd:YAG rod, through a Fresnel lens with an area of 4 m². Moreover, the highest CW solar laser power of 351.8 W was numerically achieved in 2022 [32]. In this study, a 6 mm diameter, 30 mm length Nd:YAG rod was pumped through four off-axis parabolic concentrators. For the multi beam/multi rods solar laser configuration, the maximum solar laser output power of 500 W was experimentally reached in 1993 [31], in which four Nd:YAG rods were pumped through a heliostat field-64 parabolic mirrors with total area of 3500 m².

In the present paper, we report a numerical study of high power Nd:YAG laser approach, side-pumped by solar energy through six off-axis parabolic concentrators. This laser can efficiently be used to produce energy reservoirs by exploiting the chemical potential of magnesium. Six off-axis parabolic mirrors with a total collection area of 15 m² were used as primary concentrators to collect and focus the solar energy towards six 2V-shaped pump cavities, within which a 120 mm length, 7.5 mm diameter Nd:YAG laser crystal was transversally pumped. The main advantage of the off-axis parabolic mirrors is ability to reduce losses attributed to the laser head shadow and their associated fixing mechanics when using ordinary parabolic mirrors, as well as losses stemming from the large spot size, as well as chromatic aberration at the focal zone when employing Fresnel lenses [23-25]. Six fused-silica aspheric-lenses were also employed as secondary concentrators to efficiently couple the concentrated solar power to the laser rod. All pumping parameters of the solar laser design were optimized and determined using the ZEMAX© non sequential ray-tracing method. The laser resonant cavity and its performance were analyzed and optimized by LASCAD© LASer Cavity Analysis and Design software. A maximum solar laser output power of 646 W was numerically achieved in the CW multimode operation with high collection efficiency of 43.06 W/mm².

To the best of our knowledge, this is the highest CW laser output power extracted from a single beam/single rod Nd:YAG solar laser scheme, which is more than 5 times that of the previous most powerful Nd:YAG solar laser achieved experimentally using the single rod structure [12], and 1.83 times more than the most powerful Nd:YAG solar laser obtained numerically [32]. It is also 1.29 times more than the highest solar laser power of 500 W extracted experimentally from the multi rod configuration [31]. The solar laser designed in this work can provide a laser intensity of 2.85×10^6 W/cm^2 at its focal spot, which demonstrates more than 3, 14 and 59 times the 8.34×10^5 W/cm^2 Nd:YAG solar laser flux [8], the 2×10^5 W/cm^2 CO_2 laser flux [7] and the 4.8×10^4 W/cm^2 Nd:YAG solar laser flux [6] for magnesium production efficiency.

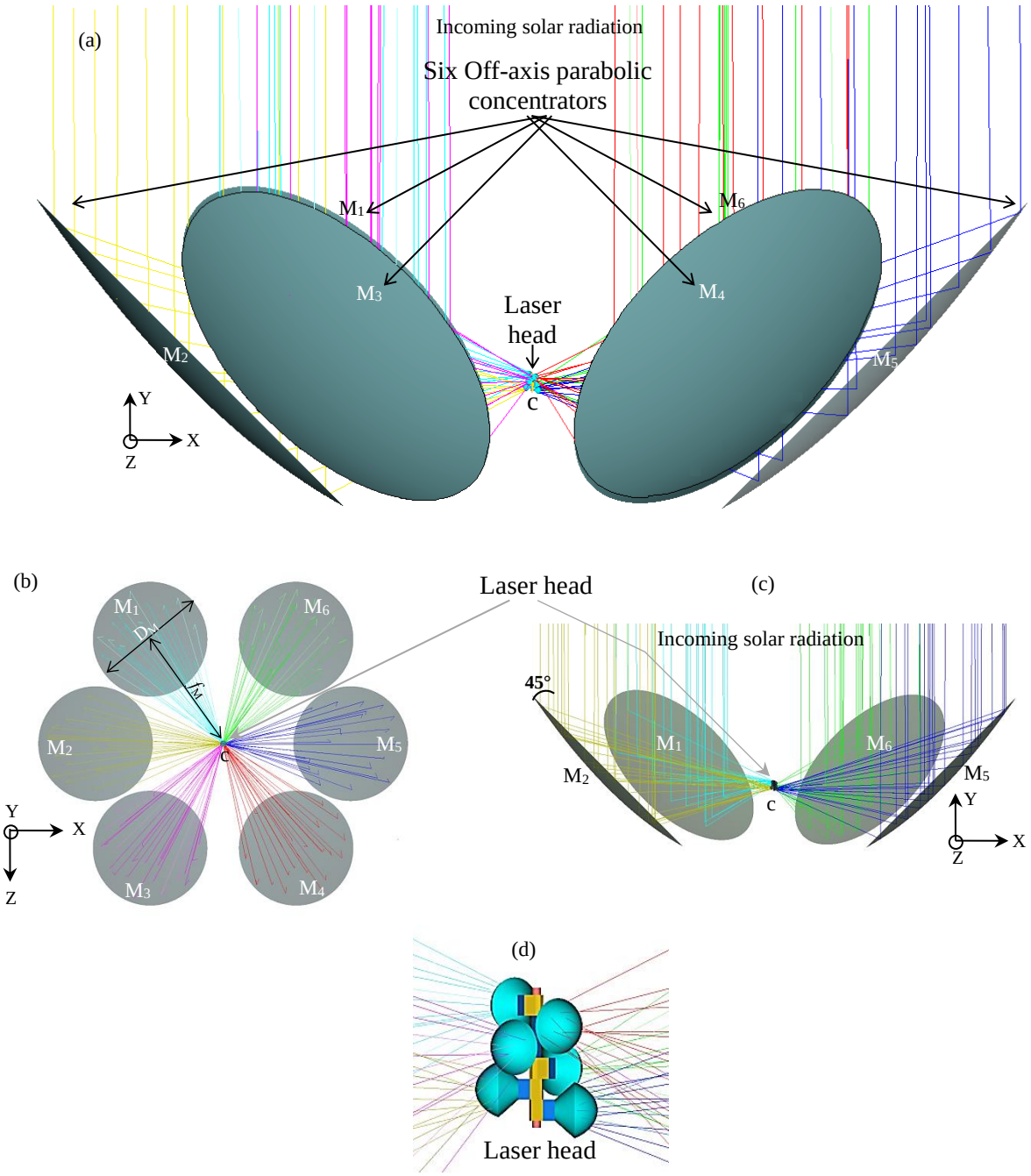

Fig. 1. Simplified scheme of a side-pumped solar laser system with six off-axis parabolic mirrors: (a) 3D general view, (b) front view, (c) side view without mirrors M_3 and M_4 to illustrate how incoming solar rays are focused towards the laser head, and (d) enlarged view of the laser head located at the point c (color online)

2. ZEMAX© design and analysis of the Nd:YAG solar laser pumped through six off-axis parabolic concentrators

2.1. Solar energy collection and concentration system

Fig. 1a shows the solar energy collection and concentration system optimized using ZEMAX© software to collect and focus the solar radiation towards the laser head at the point c. It composed of six off-axis parabolic-mirror primary concentrators (M_1–M_6). Each mirror has a diameter D_M of 1.78 m, a focal length f_M of 2 m and titled at a 45° angle relative to the Y axis as illustrated in Figs. 1b and 1c. All the primary concentrators provide a collection area of 15 m^2 and a protective silver coating of 95% reflectivity was assumed for the numerical analysis.

The main advantage of the off-axis parabolic-mirrors is the ability to eliminate completely the laser head shadowing effect and its fixation mechanics support, compared to other conventional heliostat–parabolic-mirror systems. Moreover, this kind of concentrators can significantly reduce losses in pump power due to the large spot size, as well as chromatic aberration at the focal zone when employing Fresnel lenses [23-25]. Therefore, the laser output power and efficiency can be increased. The solar laser head is fixed on an X–Y–Z axes positioner, ensuring accurate optical alignment with the parabolic mirrors.

As shown in Fig. 2, by assuming an average terrestrial solar irradiance of 950 W/m^2 on clear sunny days in Algeria, an approximate solar power of 2256 W can be focused by each off-axis mirror within a near Gaussian light spot of nearly 15 mm full width at half maximum (FWHM). This parameter is very important for the conception of the laser head and the choice of the laser medium size. Consequently, for the six primary concentrators with a total collection area of 15 m^2, about 13.5 kW was assumed to reach the laser head at their focal zones, as shown in Fig. 1.

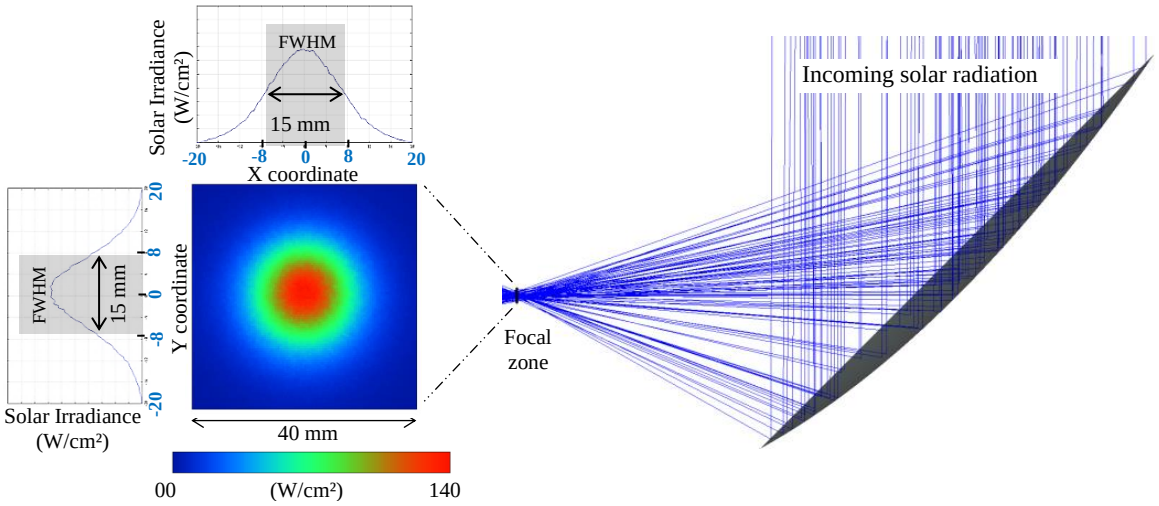

Fig. 2. Spatial distribution of the concentrated solar light at the Off-axis mirror focal zone obtained through ZEMAX© analysis (color online)

2.2. Laser Head

The solar laser head shown in Fig. 3, is composed of six fused-silica aspheric lenses used as secondary concentrators and six 2V-shaped pump cavities, wherein a single Nd:YAG laser rod with a length L_R of 120 mm and a diameter D_R of 7.5 mm was side pumped. All the parameters of the laser head were optimized using ZEMAX© software. Six fused-silica rectangular light guides were also added between each lens and the pump cavity to avoid contact between lenses. The resonant cavity consisted of two opposing mirrors. One is a 1064 nm high reflection-coated (HR 1064 nm) mirror, while the other is a 1064 nm partial reflection-coated (PR 1064 nm) mirror.

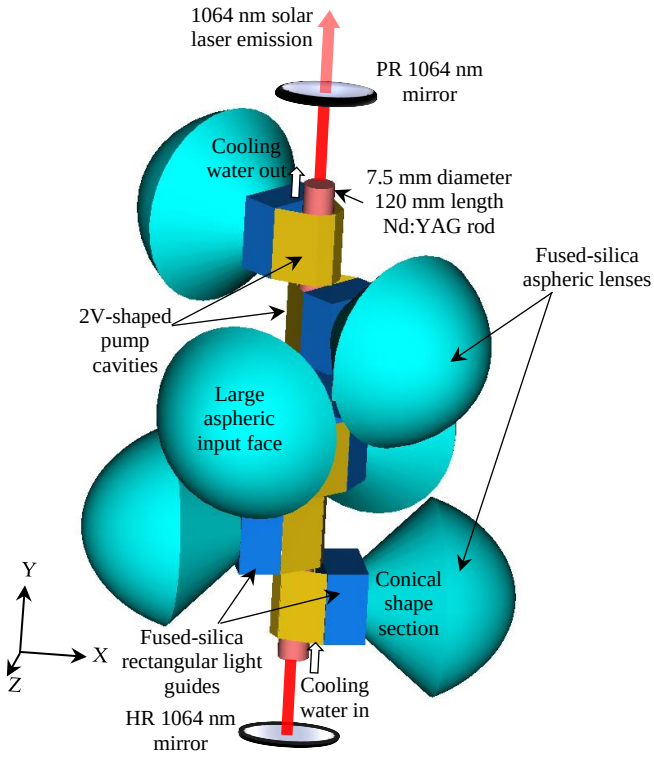

Fig. 3. Design of the Nd:YAG solar laser head, optimized with ZEMAX©(color online)

As illustrated in Figs. 4a and 4b, each fused-silica lens was optimized with a diameter of 48 mm, a radius of curvature of 26 mm, a rear conic parameter r^2 of –0.007 and a height of 37 mm. The fused-silica material was used because of its high optical and thermal properties for Nd:YAG solar laser pumping [14,33].

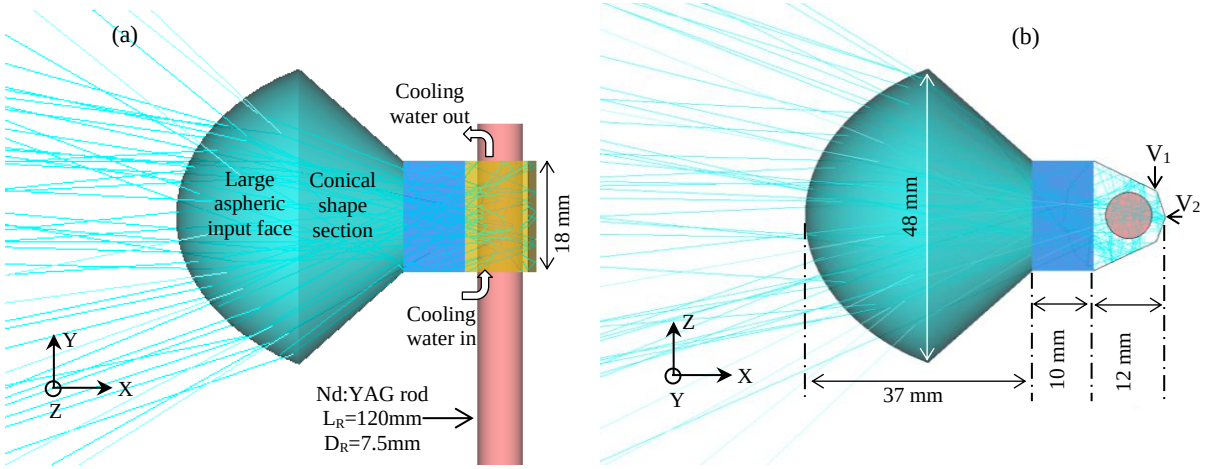

Fig. 4. Solar pumping scheme of one of the six fused-silica aspheric lenses and one 2V-shaped pump cavity: (a) front-view and (b) side-view (color online)

Each aspheric lens concentrated the solar light inside a 2V-shaped pump cavity to pump the laser rod. As depicted in Fig. 4, the pump cavity was optimized with V-shaped reflector V_1 at an angle α_1 = 130 °, and two upper plane reflectors V_2 at an angle α_2 = 140 °. The entrance aperture was then 18 mm × 18 mm, with a depth of 12 mm. The

inner wall of all the six pump cavities was assumed with a protected silver-coated aluminum foil with 95% reflectivity. This design of the laser head ensured efficient coupling of the concentrated light by the off-axis primary mirrors to the laser rod. Moreover, water-cooling at a flow rate of 6 l/min was considered to extract the heat generated along the laser rod and the pump cavities.

2.3. ZEMAX© analysis of the Absorbed Pump Power

To achieve the maximal absorbed pump power within the Nd:YAG laser rod, all the solar laser design parameters were firstly optimized using the non-sequential ray-tracing method of ZEMAX© software. 22 absorption peak wavelengths of 1.0% at. Nd^{3+} doped YAG single-crystal rod and their respective absorption coefficients were added to the glass catalogue in the ZEMAX© software [34]. The absorption spectra and refractive indexes of fused silica and water were also defined in the ZEMAX© numerical data. Moreover, the 16% overlap coefficient between the Nd:YAG absorption spectrum and the solar light spectrum was considered for the effective pump power of the solar source. Despite this small overlap value, it was confirmed that Nd:YAG is among the best laser materials solar pumping owing to its good thermal conductivity, high quantum efficiency, and high mechanical strength [11, 35]. The laser rod was divided into 49,600 voxels and the path length of each voxel was determined. To accurately compute quantitative energy distribution in the laser rod, it generally requires a larger number of rays (several millions for complex systems) [36]. In the present study ten million rays traced are used for the accuracy of the results. Then, the total absorbed solar pump power was calculated by summing the absorbed power of each voxel. Fig. 5 presents the pump-flux distribution of the absorbed power obtained using the ZEMAX© software along the central longitudinal cross –section and six transversal cross-sections of the 120 mm length, 7.5 mm Nd:YAG laser rod. About 1760 W of the solar pump power was absorbed by the laser rod.

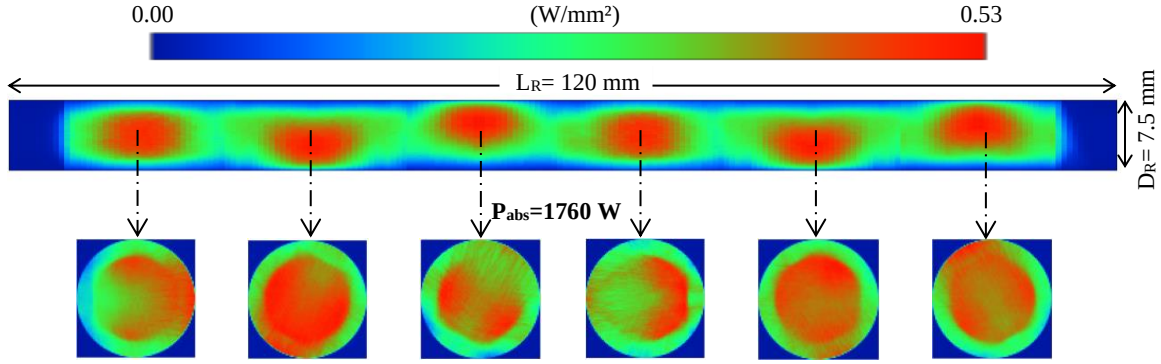

Fig. 5. Absorbed pump flux distribution inside the Nd:YAG rod with a diameter of 7.5 mm and a length of 120 mm (color online)

3. LASCAD© optimization and analysis of the laser optical resonator and output performance

The absorbed pump flux data obtained by the ZEMAX© software was then processed using the LASCAD© software to optimize the laser optical resonator and to calculate the beam output performance such as the laser power, beam quality, efficiency etc. Different parameters of the 1.0% at. Nd:YAG material were also defined in the LASCAD© software such as: the stimulated emission cross section of 2.8×10^{-19} cm^2, the fluorescence lifetime of 230 μs, a typical absorption and scattering loss of 0.003 cm^{-1}, and the average absorbed and intensity-weighted solar pump wavelength 660 nm [37].

As shown in Fig. 6, a symmetric optical resonant cavity was found as the best resonator configuration for extracting the maximum multimode laser power. It consist of a high reflection coated rear mirror (HR1064 nm, R> 98.8%) and a partial reflection coated output coupler (PR1064 nm). The two mirrors were positioned in opposing and parallel directions, at right angles to the optical axis of the laser rod. L_1 and L_2 represent the separation length of the HR mirror and the PR mirror, respectively, to the anti-reflection coating (AR) end faces of the Nd:YAG rod with 120 mm length and 7.5 mm diameter. For this symmetric optical resonator, the values of L_1 and L_2 were optimized to 149.3 mm with a radius of curvature of each mirror of + 0.2 m. Consequently, the total cavity length was $L_1 + L_2 + L_R = 418.6$ mm.

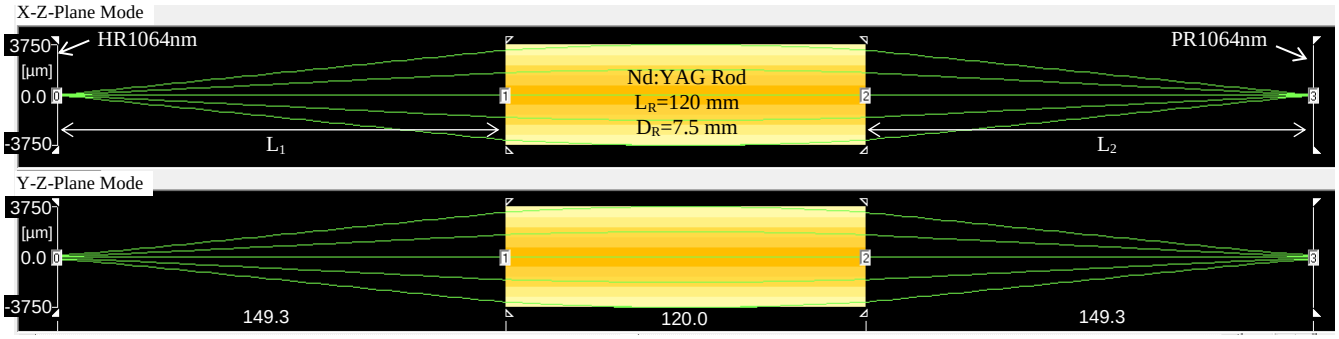

Fig. 6. Symmetric laser resonant cavity optimized by LASCAD© software for extracting the highest multimode laser output power (color online)

The solar laser output power was then calculated by considering all the losses within the laser cavity due to absorption, scattering, and diffraction phenomena. Figs. 7 and 8 illustrate the variation of the laser output power as a function of the output mirror reflectivity and the incoming solar pump power, respectively. A maximum multimode laser power of 646 W was obtained for 76% output coupler reflectivity. A solar-to-laser power conversion efficiency of 4.77% and the laser slope efficiency of 6.63% were also calculated. The laser beam quality factors was found to be M_x^2=3.3 and M_y^2 = 9.0 with a small beam spot size of about 72 μm × 314 μm.

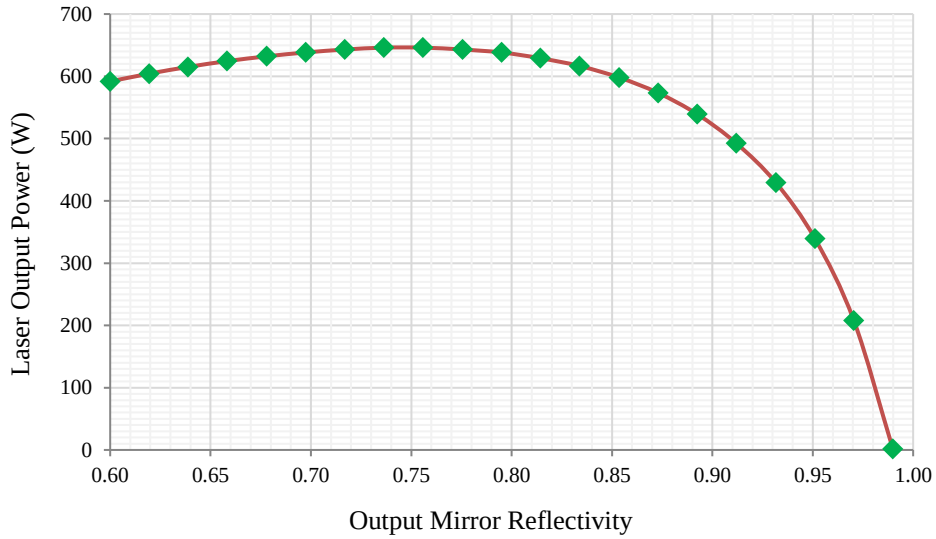

Fig. 7. Solar laser output power as a function of the output coupler reflectivity (color online)

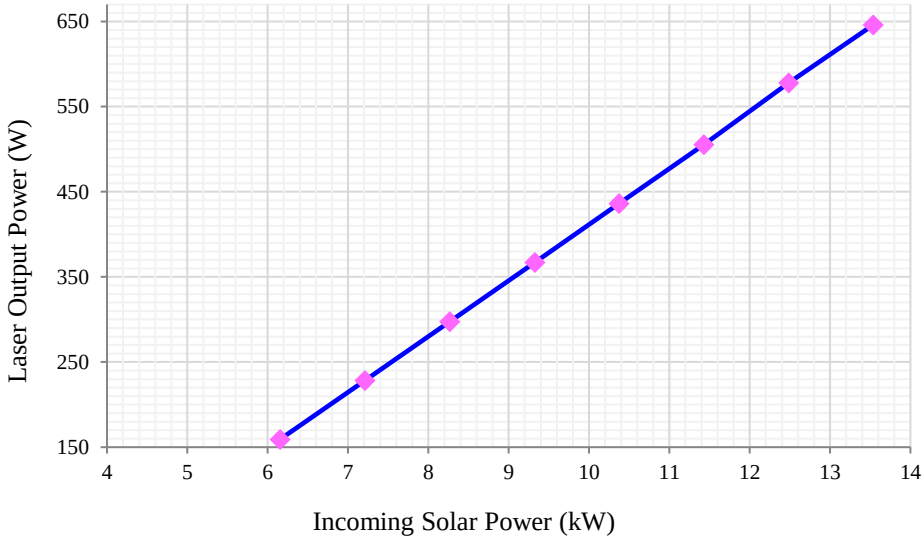

Fig. 8. Solar laser output power as a function of the incoming solar light power (color online)

As shown in Fig. 9, the laser output power variation as a function of the laser rod diameter was studied. For 120 mm rod length, an optimal value of the rod diameter was found to be 7.5 mm to extract the maximum laser power of 646 W.

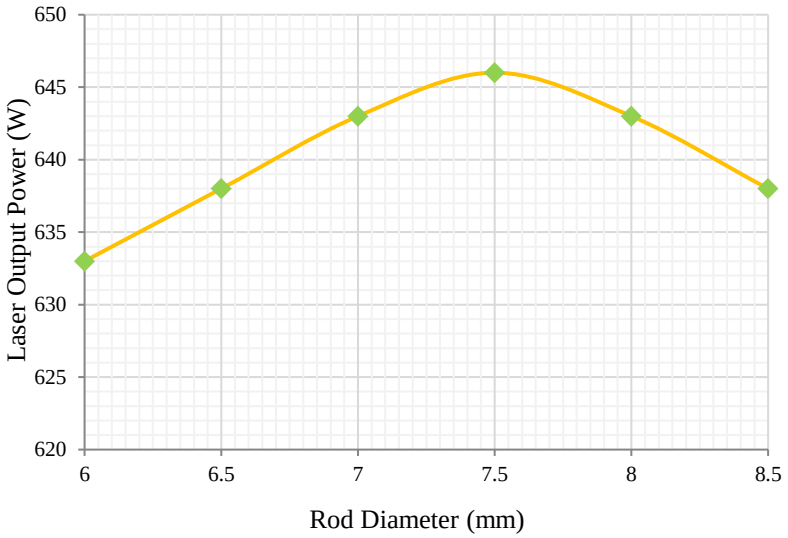

Fig. 9. Solar laser output power as a function of the Nd:YAG rod diameter (color online)

Heat load, temperature, and stress intensity distributions within the 7.5 mm diameter, 120 mm length Nd:YAG rod were also analyzed through the Finite Element Analyses (FEA) of LASCAD© software, as presented in Fig. 10. A maximum heat load of 0.47 W/mm^3 and a maximum temperature of 371.9 K were generated within the laser rod. This corresponds to a maximum thermal stress of 140.3 N/mm^2, which is considerably lower than the stress fracture limit of Nd:YAG mediums, estimated at 200 N/mm^2 [37]. Consequently, an efficient solar laser can be operated with high output power and good beam quality in the multimode operation regime.

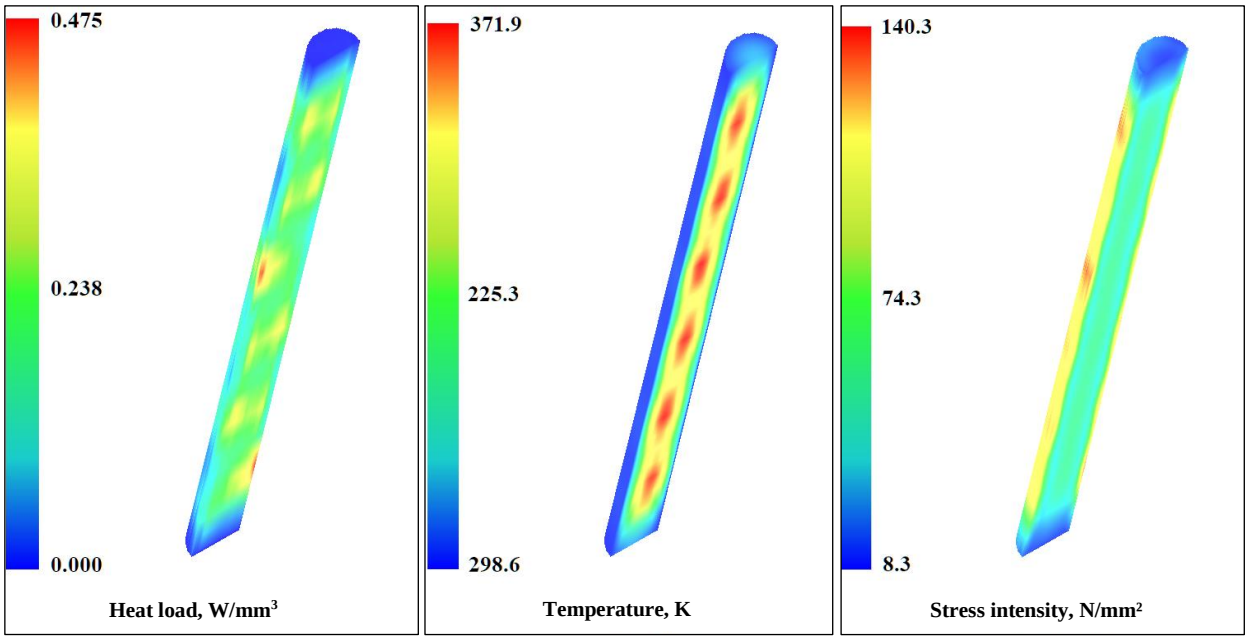

Fig. 10. Heat load, temperature, and stress intensity profiles, numerically simulated through LASCAD©-FEA analysis, for the 7.5 mm diameter, 120 mm length Nd:YAG rod (color online)

4. Discussions

With a 15 m² total collection area of the six off-axis parabolic concentrators used in this study as primary concentrators, a corresponding collection efficiency of 43.06 W/m² was achieved. This value is 1.24 times higher than our previous work using four off-axis mirrors [23]. Furthermore, the obtained laser output power of 646 W is 5.38 times more than the most powerful Nd:YAG solar laser realized experimentally, using single beam/single rod scheme [12]. It is also 1.83 times more than the highest previous numerical result of Nd:YAG solar laser, pumped through four off-axis parabolic mirrors [32]. It is also 1.29 times more than the highest solar laser power of 500 W extracted experimentally from the multi beam/multi rod configuration [31].

Additionally, the present solar laser with a beam spot size of 72 × 314 µm² at its focal zone can attain a laser intensity of 2.85×10^6 W/cm², which is more than 3, 14 and 59 times the 8.34×10^5 W/cm² Nd:YAG solar laser flux [8], the 2×10^5 W/cm² CO_2 laser flux [7] and the 4.8×10^4 W/cm² Nd:YAG solar laser flux [6] for magnesium production efficiency.

5. Conclusion

In this work, high power Nd:YAG solar laser approach, side-pumped through off-axis parabolic concentrators was presented. Six off-axis primary concentrators with 15 m² total collection area were used to collect and concentrate the solar light towards six 2V-shaped pump cavities, wherein a single Nd:YAG laser rod with 120 mm length, 7.5 mm diameter was pumped. Six fused-silica aspheric lenses were also employed to efficiently couple the concentrated solar power with a laser medium. A 646 W multimode laser power was numerically achieved as the highest value for single beam/single rod Nd:YAG solar laser scheme. This corresponds to a collection efficiency of 43.06 W/mm², which is 1.87 times more than our previous result using the same primary concentrator. Moreover, the laser power obtained here is more than 5 times that of the most powerful Nd:YAG solar laser for the single rod scheme and 1.29 times more than the highest solar laser power obtained experimentally for the multi rod configuration. A solar-to-laser power conversion efficiency of 4.77% and the laser slope efficiency of 6.63% were also calculated. The laser beam quality factors was found to be M_x^2=3.3 and M_y^2 = 9.0 with a small beam focal spot size of about 72 µm × 314 µm. This can provide a laser intensity of 2.85×10^6 W/cm² at its focal plan, which is 14 and 59 times, over the existing experimental works for laser-induced magnesium production. Therefore, this laser can efficiently be used for magnesium energy production.

Acknowledgments

Financial support for the Strategic Project UID/FIS/00068/2020 of the Science and Technology Foundation of Portuguese Ministry of Science, Technology, and Higher Education (FCTMCTES) is gratefully acknowledged.

Financial support for the Project 32/CDTA/DGRSDT/2019 of the Directorate-General for Scientific Research and Technological Development (DGRSDT) of Algerian Ministry of Higher Education and Scientific Research is gratefully acknowledged.

References

[1] S. A. Boudghene, Renewable and Sustainable Energy Reviews **15**(2), 1169 (2011).
[2] G. Kacem, B. Yahia, Journal of Renewable Energy **2013**, Article ID 496348 (2013).
[3] K. Abdeladim, S. Bouchakour, A. Hadj Arab, S. Ould Amrouche, F. Cherfa, B. Taghezouit, K. Karim, 29th European Photovoltaic Solar Energy Conference and Exhibition, Amsterdam, The Netherlands (2014).
[4] https://www.cder.dz/spip.php?article882.
[5] T. Yabe, S. Uchida, K. Ikuta, K. Yoshida, C. Baasandash, M. S. Mohamed, Y. Sakurai, Y. Ogata, M. Tuji, Y. Mori, Y. Satoh, T. Ohkubo, M. Murahara, A. Ikesue, Applied Physics Letters **89**, 261107 (2006).
[6] T. Yabe, T. Ohkubo, T. H. Dinh, H. Kuboyama, J. Nakano, K. Okamoto, in: S. N. Mathaudhu, W. H. Sillekens, N. R. Neelameggham and N. Hort (Eds.), Magnesium Technology, Springer Cham, 55–58, 2012.
[7] S. H. Liao, T. Yabe, Journal of Applied Physics **109**, 013103–9 (2011).
[8] J. Almeida, D. Liang, Proc. SPIE **9286**, 92861P (2014).
[9] M. Oliveira, D. Liang, J. Almeida, C. R. Vistas, F. Gonçalves, R. Martins, Solar Energy Materials and Solar Cells **155**, 430 (2016).
[10] C. G. Young, Applied Optics **5**(6), 993 (1966).
[11] H. Arashi, Y. Oka, N. Sasahara, A. Kaimai, M. Ishigame, Japanese Journal of Applied Physics **23**(Part1, No.8), 1051 (1984).
[12] T. H. Dinh, T. Ohkubo, T. Yabe, H. Kuboyama, Optics Letters **37**(13), 2670 (2012).
[13] J. Almeida, D. Liang, E. Guillot, Optics & Laser Technology **44**, 2115 (2012).
[14] D. Liang, J. Almeida, E. Guillot, Applied Physics B **111**, 305 (2013).
[15] D. Liang, J. Almeida, C. R. Vistas, E. Guillot, Solar Energy Materials and Solar Cells **159**, 435 (2017).
[16] D. Liang, C. R. Vistas, B. D. Tiburcio, J. Almeida, Solar Energy Materials and Solar Cells **185**, 75 (2018).
[17] D. Liang, J. Almeida, B. D. Tibúrcio, M. Catela, D. Garcia, H. Costa, C. R. Vistas, Journal of Solar

Energy Engineering **143**, 061004 (2021).
[18] D. Liang, C. R. Vistas, D. Garcia, B. D. Tibúrcio, M. Catela, H. Costa, E. Guillot, J. Almeida, Solar Energy Materials and Solar Cells **246**, 111921 (2022).
[19] D. Liang, J. Almeida, M. Catela, H. Costa, D. Garcia, B. D. Tibúrcio, E. Guillot, C. R. Vistas, Solar Energy Materials and Solar Cells **270**, 112817 (2024).
[20] R. Bouadjemine, D. Liang, J. Almeida, S. Mehellou, C. R. Vistas, A. Kellou, E. Guillot, Optics & Laser Technology **97**, 1 (2017).
[21] S. Mehellou, D. Liang, J. Almeida, R. Bouadjemine, C. R. Vistas, E. Guillot, F. Rehouma, Solar Energy **155**, 1059 (2017).
[22] R. Boutaka, R. Bouadjemine, D. Liang, N. Hendaoui, A. Kellou, Journal of Physics: Conference Series **1859**, 012057 (2021).
[23] R. Boutaka, R. Liang, R. Bouadjemine, M. Traiche, A. Kellou, Journal of Russian Laser Research **42**(4), 453 (2021).
[24] R. Boutaka, D. Liang, A. Kellou, Journal of Photonics for Energy **12**(3), 038002, 1 (2022).
[25] R. Boutaka, D. Liang, R. Bouadjemine, N. Hendaoui, Optical Engineering **63**(6), 066101 (2024).
[26] P. Guo, J. Zhang, Z. Chen, L. Lan, Y. Liu, Y. Tang, X. Ma, Optik **271**, 170096 (2022).
[27] C. Zitao, Z. Changming, Z. Ziyin, J. Zhang, Z. Zhang, H. Zhang, Optics Express **2**(31), 1340 (2023).
[28] W. Biqing, L. Lanling, L. Yan, T. Yulong, Z. Yuanyuan, Journal of Russian Laser Research **44**(6), 682 (2023).
[29] Q. Hongfei, L. Yan, L. Lanling, Z. Yuanyuan, M. Xiuhua, Applied Solar Energy **60**(1), 83 (2024).
[30] A. Sherniyozov, S. Payziyev, S. Begimqulov, Journal of Photonics for Energy **14**(2), 024501 (2024).
[31] V. Krupkin, Y. Kagan, A. Yogev, Proc. SPIE **2016**, 50 (1993)
[32] Q. Hongfei, L. Lanling, L. Yan, X. Pengfei, T. Yulong, Current Optics and Photonics **6**(6), 627 (2022).
[33] www.newport.com/n/optical-materials.
[34] Standard Tables for Reference Solar Spectral Irradiances: Direct, Normal, and Hemispherical on 37◦ Tilted Surface, ASTM Standard G173–03 (2012).
[35] Z. Bin, C. Zhao, J. He, S. Yang, Acta Optica Sinica **27**, 1797 (2007).
[36] D. Liang, J. Almeida, C. Vistas, B. D. Tibúrcio, D. Garcia, Solar-Pumped Lasers: With Examples of Numerical Analysis of Solid-State Lasers, Springer Cham, Switzerland (2023).
[37] W. Koechner, Solid-State Laser Engineering, 6th ed. Springer, Berlin 1999.

*Corresponding author: rboutaka@cdta.dz